Aalborg Universitet

AALBORG UNIVERSITY

The Impact of Mission Profile Models on the Predicted Lifetime of IGBT Modules in the Modular Multilevel Converter

Zhang, Yi; Wang, Huai; Wang, Zhongxu; Yang, Yongheng; Blaabjerg, Frede

The Impact of Mission Profile Models on the Predicted Lifetime of IGBT Modules in the Modular Multilevel Converter

Yi Zhang, Huai Wang, Zhongxu Wang, Yongheng Yang, Frede Blaabjerg
Department of Energy Technology, Aalborg University, Aalborg, Denmark
yiz@et.aau.dk, hwa@et.aau.dk, yoy@et.aau.dk, zho@et.aau.dk, fbl@et.aau.dk

Abstract—The reliability aspect study of Modular Multilevel Converter (MMC) is of great interest in industry applications, such as offshore wind. Lifetime prediction of key components is an important tool to design MMC with fulfilled reliability specifications. While many efforts have been made to the lifetime prediction of IGBT modules in renewable energy applications by considering long-term varying operation conditions (i.e., mission profile), the justifications of using the associated mission profiles are still missed. This paper investigates the impact of mission profile data resolutions and electrical power modeling methods on the estimated lifetime of IGBT modules in an MMC for offshore wind power application. In a 30 MW MMC case study, an annual wind speed profile with a resolution of 1 s/data, 10 minute/data, and 1 hour/data are considered, respectively. A method to re-generate higher resolution wind speed data from lower resolution data is introduced as well. Based on the wind speed data, IEC 61400-12-1 power curve model and a wind speed-power stochastic model are compared as well. Five mission profile modeling scenarios are compared in terms of the predicted lifetime of the IGBT modules used in the MMC, resulting in significant differences. The study serves as a first step to quantify the impact of mission profile modeling on lifetime prediction, and to provide a guideline on mission profile collection for the presented application.

I. INTRODUCTION

The Modular Multilevel Converter (MMC) is one of the most attractive topologies for medium and high power applications, especially for High-Voltage Direct Current (HVDC) transmission systems to connect offshore wind farms to the grid [1], [2]. Until now, in Germany, eight MMC-based HVDC systems that connect offshore wind farms to the main grid have been installed [3], where the maximum power of an MMC-based HVDC project is up to 900 MW.

In literature, many research efforts have been devoted to the basic operation and control of MMC systems [1]. For instance, in [4], the capacitor voltage balancing control has been discussed; in [5], the steady-state model of the MMC has been built; and in [6], [7], the modulation algorithms have been analyzed and improved. However, as MMCs are the key for HVDC systems, which are exposed to harsh environmental conditions, reliability has become a major concern in MMC-based HVDC systems. In order to meet the reliability requirements, the component-level reliability analysis should be performed first, and also widely explored in other power electronic systems (e.g., PV applications). Additionally, the high-reliability demand also comes from the fact that the
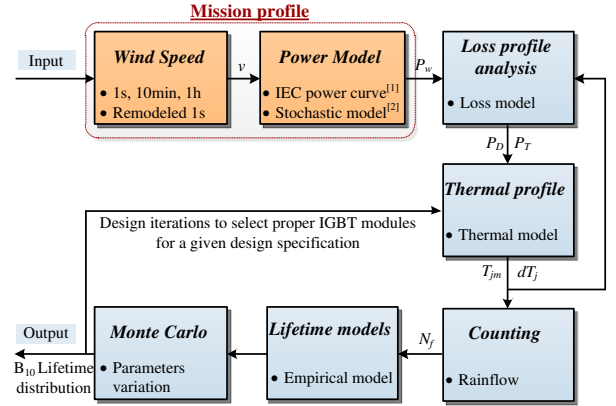

Fig. 1: Mission profile based lifetime estimation method for IGBT modules in the MMC.

power electronic device (e.g., IGBT modules), ranked as the highest failure rate in an industry survey [8].

Regard to reliability analysis, in [9], [10], the IGBT-module lifetime of the MMC is estimated based on constant failure rates. However, the used concept of Mean Time to Failure (MTTF) is outdated, as the failure rate over the operational time is not constant in practical cases. In contrast, the mission profile based lifetime estimation method (as shown in Fig. 1) considers real working environment conditions. Thus, it has been widely accepted in wind turbines (WTs), and photovoltaic (PV) systems. In [11], the mission profile based lifetime estimation method is proposed for the IGBT modules of the MMC, but the justification of a specific mission profile with the resolution of 1 hour/data is not discussed. Beyond MMC applications, the impact of the mission profile data resolution is neither addressed in many other cases, like WTs. In the other words, the impact of the resolution of mission profiles on the reliability prediction of power electronic systems is still unclear. In light of the above issues, this paper explores the impacts of mission profile resolution on the lifetime prediction of the MMC systems. In addition, different power conversion models are considered in the analysis.

As illustrated in Fig. 1, the mission profile in this case consists of an annual wind speed and a power conversion model, to produce power fed into MMC-lifetime calculation. This study

aims to determine the impact of both the resolution of wind speeds and the selection of power conversion models. Based on the outcome, a corresponding requirement for mission-profile models can be clarified. Inspired by that, annual wind speeds with different resolutions (1 s/data, 10 minute/data, 1 hour/data and a remodeled 1 s/data) and two wind speed - electrical power conversion models are implemented into a 30MW MMC.

The outline of this paper is as follows. Section II briefly introduces the mission profile based lifetime prediction method. Section III presents the quantitative impact analysis for a 30 MW MMC case study with five mission profile modeling scenarios, followed by the conclusions.

II. MISSION PROFILE BASED LIFETIME PREDICTED METHOD

Mission profile based lifetime estimation has gained much popularity for reliability analysis in power electronic systems. In wind power applications, a translation from the mission profile to output power, losses, thermal cycles, and finally to obtain the lifetime consumption of components or the entire system should be performed. However, the requirements of the mission profile data resolution are not addressed in previous literature. Higher mission profile data resolution could ensure higher accuracy in lifetime prediction since it incorporates more rich information in dynamics, however, at the expense of more efforts to data measurement, storage, and and analysis. It is still an open question what is the required mission profile data resolution to achieve an acceptable uncertainty level in lifetime prediction of power electronic components.

Inspired by the estimated lifetime may change, depending on the different mission profile models. This study adopts 1-year wind-speed data from an offshore wind farm with different resolutions (1 s/data, 10 minute/data, 1 hour/data, and a remodeled virtual 1 s/data), then two different power conversion models are employed to translate the mission profile into the output power of a wind farm (i.e. IEC power curve, stochastic model), in order to compare the impact on the estimated lifetime.

The details of the mission profile based lifetime prediction method are introduced as follow:

A. Mission Profile Model

When the MMC collects the wind power from an offshore wind farm, the platform is exposed to harsh environments. However, due to the offshore MMC platform must be maintained to specified levels of temperature, humidity, and pressure inside the platform [3], the dominant stress for power devices of MMC is due to the power fluctuation of the wind farm. Unfortunately, the actual long-term power fluctuations are usually unaccessible during the products design. In order to estimate the lifetime of the MMC, an annual wind speed is adopted as a representative long-term profile for analysis. Then, the power fluctuations based on the annual wind speed are modeled following the two steps:

1) Mission profile in a specific location with a specific resolution: higher resolution means less information loss but at the cost of increased calculation. However, high-resolution mission profile such as 1 s/data is not common. In that case, 10 minute/data or 1 hour/data mission profiles are utilized as substitute. In addition, regeneration models are also alternative to remodel the dynamics at the time scale of 1s, to produce the remodeled 1 s/data profiles.

2) Mission profile translation into the output power of the wind farm: the simplest model to describe the process from the wind speed to the output power of a wind farm is to look up IEC power curve according to IEC 61400-12-1 [12], which is originally designed for a single wind turbine. This power curve is widely accepted by most wind-turbine manufacturers, but it only reveals the steady-state output power. When this model is employed to describe the output power of the entire wind farm, it may induce some errors due to the neglecting of dynamics and turbulences of the wind farm. Alternatively, a stochastic model [13] was thus proposed to describe the conversion process of a wind farm at the 1 s/data wind speeds. This model has been validated by the measured data from a wind farm. It should be noted that when the wind speed is sampled at longer time scale (i.e., 10 minute/data or 1 hour/data), the dynamic effects of wind farm is alleviated. The output power of the wind farm can be looked up from the IEC power curve directly.

Therefore, four wind-speed profiles (i.e., 1 s/data, 10 minute/data, 1 hour/data, and a remodeled virtual 1 s/data), and two power conversion models (IEC power curve and stochastic model) are implemented as the mission profiles. Due to the 1 s/data wind speed has the highest resolution and the stochastic model has been validated by the actual wind farm, this paper benchmarks their lifetime results.

B. Power Loss Profile

According to the output power of a wind farm, a mapping relationship between the loss profile of power devices and power fluctuations can be obtained. In this paper, in order to obtain an accurate loss profile, a three-dimension lookup table will be built up based on a detailed simulation model in PLECS. All the conduction losses, switch-on losses, switch-off losses, and recovery losses are taken into this model account.

C. Thermal Profile

The dominant failure mechanism of the MMC is the temperature swings generated by losses, then the key question is how to map the power losses to the thermal profile, where an appropriate thermal model should be adopted. Foster and Cauer models are two typical thermal models. The Cauer model is built up on physical parameters of power devices. These parameters are not provided in the data sheet and only accessible for manufacturers. Thus, the curve fitting based Foster model is adopted here, which is shown in Fig. 2.

In this paper, an iterative analytical model [15] based on the Foster network is utilized to estimate the thermal profile from the power losses. This model considers the thermal impedance
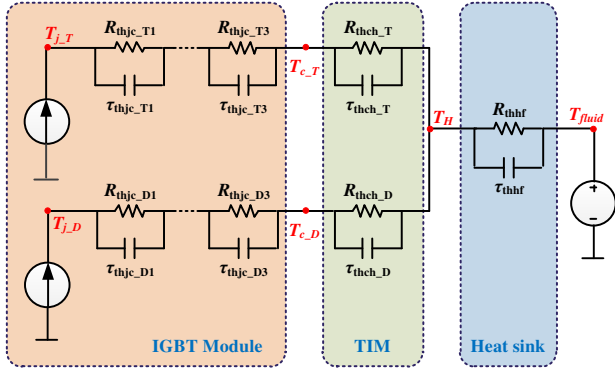
Fig. 2: Foster thermal model for IGBT modules, where the parameters from junction to case and thermal grease are listed in [14], the thermal resistance and thermal time constant of heat sink are R_{thhf} = 10 K/kW and τ_{thhf} = 127 s, respectively.

variation with a time scale equal to the resolution of mission profile (T_s), thus the dynamics of thermal response will be reflected in the results. Simply summarized, the iterative equation of the model is,

$$\Delta T_{n-1} = P_{n-1} \cdot R_{th} \cdot \left(1 - e^{-T_s/\tau}\right) \tag{1}$$

$$\Delta T_n = \Delta T_{n-1} e^{-T_s/\tau} + P_n \cdot R_{th} \cdot \left(1 - e^{-T_s/\tau}\right) \tag{2}$$

where the previous P_{n-1} and the actual dissipated power P_n in each time step are involved, and τ is the thermal time constant.

D. Power Cycling Counting

Following, the irregular thermal profile needs to be decomposed. Various counting methods includes level-crossing counting, peak counting, simple-range counting, rang-pair counting, and rain-flow counting [16]. In [17], different counting algorithms has been compared and concluded that rainflow counting algorithm has minimum errors in most cases. Therefore, the rainflow counting algorithm is adopted in this paper.

E. Lifetime Model and Monte Carlo Simulation

After the cycling counting completed, the lifetime of power modules can be estimated according to corresponding lifetime models. These lifetime models can be classified into two categories. The first one is based on the mathematical fitting of accelerated data, represented as analytical models [18], [19]. The second category includes the physics-of-failure (PoF) lifetime models [20], which requires detailed information of the materials and geometries of power semiconductor devices.

In this paper, a series of accelerated lifetime data [21] provided by the manufacturer is utilized for lifetime estimation. The counted thermal cycles are mapped by looking up the aging data rather than employing any lifetime models, thereby errors induced by curve fitting can be avoided. Then the 10% failure rate (B_{10} lifetime) can be obtained by a corresponding number of thermal cycles. The total lifetime consumption of one year CL_{1year} can be accumulated according to the
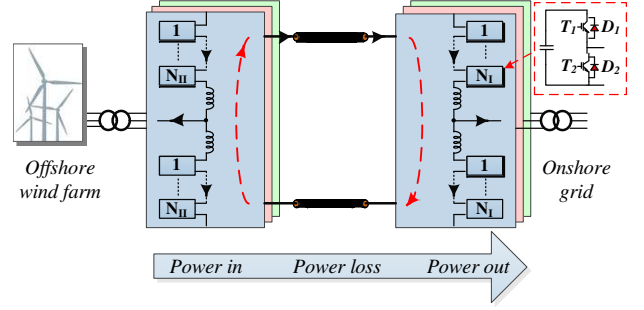

Fig. 3: A 30 MW MMC-HVDC transmission system for offshore wind power applications, where the inverter-side MMC is studied.

Palmgren-Miners rule [22] and the lifetime of the devices LF are obtained as,

$$CL_{1year} = \sum \frac{100}{N_{1\_life}} + \frac{100}{N_{2\_life}} + \cdots + \frac{100}{N_{n\_life}} \,(\%) \tag{3}$$

$$LF = \frac{1}{CL_{1year}} \tag{4}$$

Finally, parameter variations are considered through the Monto Carlo simulation [23]. A distribution of end-of-life (EOF) of power semiconductor devices are plotted, rather than a fixed accumulated damage, which allows the designer to select the most cost-effective components.

III. CASE STUDY ON A 30MW MMC

A case study of a 30 MW MMC is discussed in this section, which is utilized to connect the offshore wind farm. The mission profiles are modeled by four different resolution wind speeds and two power conversion models. Each mission profile is estimated by the same procedure mentioned in the previous section. The only difference in mission profile is aimed to clarify how to collect data and how to model the mission profile.

As shown in Fig. 3, a MMC-based HVDC transmission system for an offshore wind power application is considered, where both the rectifier side and the inverter side are three-phase MMCs. In this paper, the inverter side is selected as the case study only. In each phase of the MMC, 24 identical half-bridge sub-modules (HB-SMs) are cascaded. Each SM consists of two IGBT modules from ABB 5SNA1200E450350 [14], that is, the upper IGBT (denoted as T_1 and D_1) and lower IGBT (T_2 and D_2). The system specifications are listed in Table I. For the wind farm, 10 wind turbines (WTs) V90 [24] with 3-MW rated power are chosen in the study case.

A. Five Mission Profiles for the MMC

Mission profile is the input of the lifetime prediction method, which consists of the wind speed and a power conversion model in this case, as shown in the dashed box of Fig. 1.

The wind speed data was collected from an offshore platform in the North Sea. The data is recorded from September

TABLE I: Specifications of the Studied MMC System

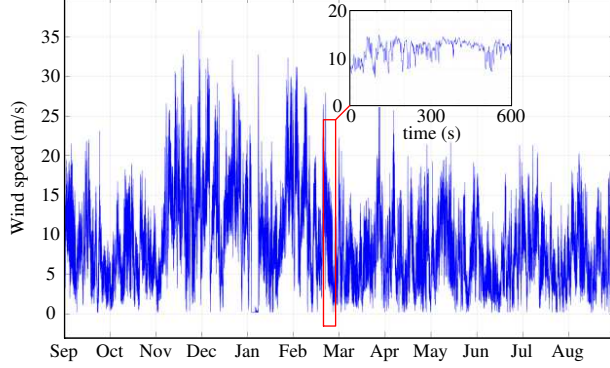| Parameters	Values
System rated active power	$P = 30$ MW
Rated DC-link voltage	$V_{dc} = 31.8$ kV
Rated AC grid voltage	$V_{ac} = 14$ kV
Number of sub-module per arm	$N = 12$
Arm inductor	$L_{arm} = 4$ mH
Arm resistor	$R_{arm} = 0.0628\Omega$
Sub-module capacitor	$C_{SM} = 0.8$ mF
Switching frequency	$f_s = 1$ kHz
Fundamental frequency	$f = 50$ Hz
Modulation index	$m = 0.9$
Power factor	PF = 1

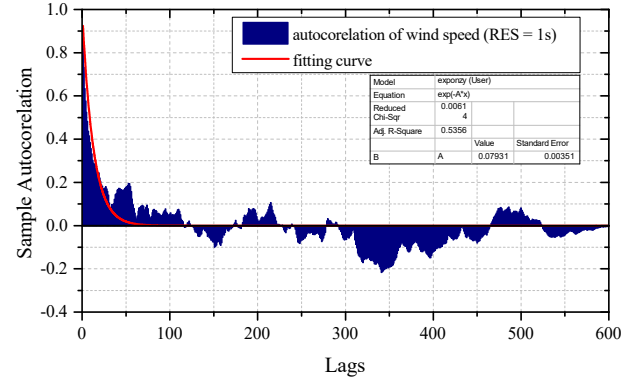Fig. 4: One-year wind speed with 1 s/data from an offshore platform.

Fig. 5: The autocorrelation of the studied wind speed, where the result of curve fitting can be utilized to regenerate high-resolution wind speed.

TABLE II: Specifications of the Studied MMC System

No.	Mission Profiles	Wind Resolution	Power Conversion Model
1	IEC1s	1 s/data	IEC power curve [12]
2	STO1s	1 s/data	Stochastic model [13]
3	IEC10min	10 minute/data	IEC power curve
4	IEC1h	1 hour/data	IEC power curve
5	STO1sREG	remodeled 1 s/data	Stochastic model

2015 to August 2016 with the resolution of 1 s/data at 80-meter height as shown in Fig. 4. The annual average wind speed is 8.7786 m/s, which belongs to the IEC Wind Class I with an average wind speed of 8.5-10 m/s. Then, the 10 minute/data and a 1 hour/data wind profiles can be obtained. Afterwards, five different mission profile models are introduced:

1) Wind Profile at 1 s/data and IEC Power Curve: the sampled annual wind profile at 1 s/data is converted by the simplest model IEC power curve [24]. The cut-in wind speed of the utilized IEC power curve is 3.5 m/s, and the rated speed is achieved roughly at 15.5 m/s. The total power production from the wind farm $P_{IEC}(u(t))$ is only obtained by multiplying the number of WTs (i.e., 10 in this case). Therefore, a conversion process from the instantaneous wind speed $u(t)$ to wind farm production P_{IEC} is modeled. Notably, other information of wind farms (e.g., dynamics, fluctuations, wind directions, etc.) is ignored in the IEC power curve.

2) Wind Profile at 1 s/data and Stochastic Model: in the field measurement [13], the 1-s/data output wind farm fluctuates around IEC power curve with deviations up to $\pm 20\%$. This reveals that large errors will be generated with the IEC power curve for power estimation in 1 s/data profile. An alternative stochastic model was proposed in [13] to solve this issue. The wind farm is considered as a dynamic system in the model, quantifying the impacts of both wind speed and additional turbulent fluctuations. When it is compared with measured signal, this model proved a good statistical

agreement, including the intermittent and gusty features. With this consideration, the mission profile based on 1 s/data wind speed and the stochastic model is benchmarked. The stochastic model can be simplified as,

$$
\begin{aligned}
\frac{dP_{STO}(t)}{dt} =& \alpha_0 \cdot P_{IEC}(u(t)) \cdot [P_{IEC} - P_{IEC}(u(t))] \\
& + \sqrt{\beta_0} \cdot P_{IEC}(u(t)) \cdot \Gamma(t)
\end{aligned} \quad (5)
$$

where the α_0 describes the attraction towards the power curve, and the β_0 quantifies additional turbulence fluctuations. For simplification, the two parameters are $\alpha_0 \approx -(6.48 \pm 0.25) \times 10^{-4}\%^{-1}s^{-1}$ and $\beta_0 \approx (7.42 \pm 0.21) \times 10^{-5}\%^{-1}s^{-1}$. P_{STO} is the output power of the wind farm based on the stochastic model, $\Gamma(t)$ represents the Gaussian-distributed noise that is not correlated.

3) Wind Profile at 10 minute/data and IEC Power Curve: to compare the impacts of wind-profile resolution, an annual 10-minute/data wind speed is obtained. Afterwards, due to the dynamic are alleviated in the time scale of 10 minutes, the output power of wind farm can be looked up from the IEC power curve directly.

4) Wind Profile at 1 hour/data and IEC Power Curve: similarly, an annual 1 hour/data wind profile is obtained. In this time-scale, most study cases employed the IEC power curve [11], [25], since the time-scale of turbulence and inertia effects is far smaller than 1 hour.

5) Remodeled 1-s/data Wind Profile and Stochastic Model: due to the limits of data storage, 10 minute/data wind speeds and its deviations are most adopted recorded type. 1 s/data profile is not accessible in most situations. However, as shown
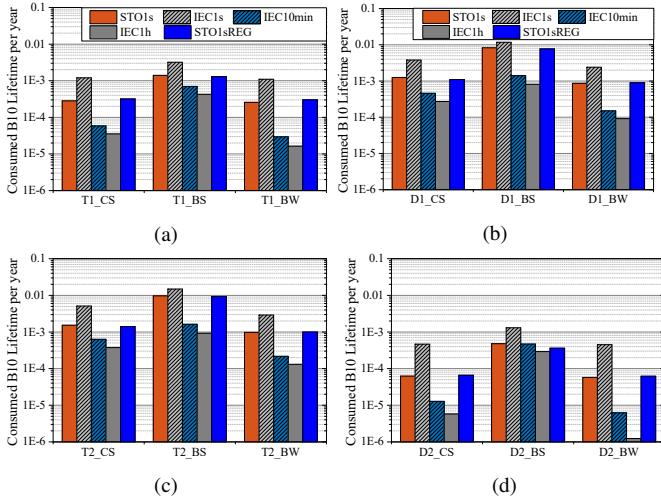
Fig. 6: The consumed B_{10} lifetime per year of four power devices in a SM of the MMC, where T_1 and D_1 means the upper IGBT and its free-wheeling diode, while T_2 and D_2 means the lower IGBT module in a SM, respectively. CS, BS and BW represent the chip solder, the baseplate solder and the bond wire respectively. (a) T_1; (b) D_1; (c) T_2; (d) D_2.

in the zoom-in box of Fig. 4, speed fluctuates during the time-scale of 10-minute, which may lead to fatigue of power semiconductor devices. In order to model wind dynamics at the time-scale of 1-second, a regenerated model from the 10 minute/data profile has been presented in [13], where the high resolution wind speed is decomposed as

$$u(t) = \overline{u} + \sigma \cdot u^{'}(t) \tag{6}$$

where $\overline{u}$ and σ are the 10 minute/data value and the standard deviation of the wind speed. The wind fluctuation signal $u^{'}$ can be modeled as

$$\frac{du^{'}(t)}{dt} = -\gamma \cdot u^{'}(t) + \sqrt{\gamma} \cdot \Gamma(t) \tag{7}$$

where γ represents the inherent characteristics of the wind farm, which needs to be trained by a period time of 1 s/data wind speed. An approximated relation of autocorrelation function of $u^{'}(t)$, that is, $R_{u^{'}u^{'}}(\tau) \approx \exp(-\gamma \cdot \tau)$. In this study, a fragment of high resolution wind speed is adopted to fit the value of γ. As shown in Fig. 5, γ is fitted as 0.07931.

In summary, five different mission profile models are listed in Table II.

B. Translation from Power Losses into Lifetime Consumption

Afterwards, different mission profile models are repeated in the procedure of Section II. The consumed B_{10} lifetime per year based on 1 s/data wind speed and stochastic model is benchmarked, then the consumed B_{10} lifetime per year based on other mission profiles will be compared with the benchmark.

As shown in Fig. 6, the lifetime consumption of IGBT chips (T_1 and T_2) and Diode chips (D_1 and D_2) have been

analyzed separately, where the CS, BS, and BW represent the three different dominant failure locations (chip solders, baseplate solders, and bond wires, respectively). The lifetime consumption based 1 s/data profile and IEC power curve is overestimated compared with the benchmark. The maximum difference is up to roughly 10 times at the bond wire of D_2 in Fig. 6(d). It reveals that large wind fluctuations at the time scale of 1s have been induced directly into power production by IEC power curve, thus impractical fatigues are calculated by this power conversion model. IEC power curve is established in the assumption of the steady state, but the time scale of 1s obviously less than the time constant of the steady state. Therefore, IEC power curve can not be accepted in 1 s/data wind speed. In addition, it is obvious that the discrepancies of baseplate solders are smaller than in chip solders or bond wires. This is because a portion of false high-frequency fluctuations can be filtered by thermal capacitance. Then the calculated fatigue is closer to the benchmark than in other two locations.

On the other hand, contrary results happens in 10 minute/data and 1 hour/data wind speed based on IEC power curve. Both their predicted lifetime consumption are underestimated. This is due to enormous several-seconds temperature swings in field operation are ignored in the mission profiles at the time scale of 10-minute or 1-hour. Hence, mission profiles based on 10 minute/data or 1 hour/data wind speed lead to longer predicted lifetime.

Finally, under the mission profile consisting of the remodeled 1 s/data wind speed and stochastic model, the predicted lifetime consumption per year is extremely closed to the benchmark. This is proved that the dynamics at 1s can be good modeled by the regenerated model. Therefore, when the information of wind speed sampled at 1s is not accessible, the regenerated high-frequency wind speed is an alternative solution.

In summary, IEC power curve induces abundant illusory high-frequency temperature swings at the 1 s/data wind speed, thus the predicted lifetime consumption of components is overestimated. On the contrary, temperature swings at seconds will be ignored by the mission profiles based on the 10 minute/data or 1 hour/data wind speed and IEC power curve, then the predicted lifetime will be longer than the benchmark. When 1 s/data wind speed is absent, a remodeled 1s/data is an alternative solution to model the lifetime consumed in the time scale of seconds.

IV. CONCLUSION

A quantitative analysis of the impact of mission profile modeling on the predicted IGBT module lifetime is presented. In a case study of 30 MW MMC for offshore wind application, five mission profiles are compared based on annual wind speed profiles with data resolutions of 1 s/data, 10 minute/data (i.e., from standard SCADA system), and 1 hour/data, and IEC 61400-12-1 power curves and a wind speed-power stochastic model. Based on the quantitative results discussed in Section III, it can draw the following conclusions:

1) Wind speed profiles with 10 minute/data and 1 hour/data do not have sufficient resolution to incorporate relatively high-frequency power cycling with cycle period in the range of seconds, resulting in underestimation of the annual lifetime consumption (i.e., overestimation of lifetime).

2) IEC 61400-12-1 power curves are not suitable to convert high resolution wind speed data (i.e., 1s/data) to generator output power, since they are based on steady-state and no mechanical inertia are considered, resulting in overestimation of the annual lifetime consumption with 1 s/data wind speed profile.

3) The difference in the predicted lifetime introduced by the three different wind speed resolutions is less for the baseplate solder of the IGBT module compared to that for the chip solder and bond wires, which is due to the fact that baseplate solder has higher thermal capacitance compared to other two sites and is less sensitive to high-frequency dynamics.

4) A re-configured 1 s/data wind speed profile based on 10 minute/data from standard SCADA systems and a stochastic model achieves acceptable lifetime prediction results.

References

[1] H. Akagi, "Classification, terminology, and application of the modular multilevel cascade converter (MMCC)," *IEEE Trans. Power Electron.*, vol. 26, no. 11, pp. 3119–3130, Nov. 2011.

[2] S. Debnath, J. Qin, B. Bahrani, M. Saeedifard, and P. Barbosa, "Operation, control, and applications of the modular multilevel converter: a review," *IEEE Trans. Power Electron.*, vol. 30, no. 1, pp. 37–53, Jan. 2015.

[3] K. Sharifabadi, L. Harnefors, H.-P. Nee, R. Teodorescu, and S. Norrga, *Design, Control and Application of Modular Multilevel Converters for HVDC Transmission Systems*. John Wiley & Sons, 2016.

[4] M. Hagiwara and H. Akagi, "Control and experiment of pulsewidth-modulated modular multilevel converters," *IEEE Trans. Power Electron.*, vol. 24, no. 7, pp. 1737–1746, Jul. 2009.

[5] K. Ilves, A. Antonopoulos, S. Norrga, and H. P. Nee, "Steady-state analysis of interaction between harmonic components of arm and line quantities of modular multilevel converters," *IEEE Trans. Power Electron.*, vol. 27, no. 1, pp. 57–68, Jan. 2012.

[6] Q. Tu, Z. Xu, and L. Xu, "Reduced switching-frequency modulation and circulating current suppression for modular multilevel converters," *IEEE Trans. on Power Del.*, vol. 26, no. 3, pp. 2009–2017, Jul. 2011.

[7] B. Li, R. Yang, D. Xu, G. Wang, W. Wang, and D. Xu, "Analysis of the phase-shifted carrier modulation for modular multilevel converters," *IEEE Trans. Power Electron.*, vol. 30, no. 1, pp. 297–310, Jan 2015.

[8] S. Yang, A. Bryant, P. Mawby, D. Xiang, L. Ran, and P. Tavner, "An industry-based survey of reliability in power electronic converters," *IEEE Trans. Ind. Appl.*, vol. 47, no. 3, pp. 1441–1451, May/Jun. 2011.

[9] J. Xu, P. Zhao, and C. Zhao, "Reliability analysis and redundancy configuration of MMC with hybrid submodule topologies," *IEEE Trans. Power Electron.*, vol. 31, no. 4, pp. 2720–2729, Apr. 2016.

[10] J. Guo, J. Liang, X. Zhang, P. Judge, X. Wang, and T. Green, "Reliability analysis of MMCs considering sub-module designs with individual or series operated IGBTs," *IEEE Trans. Power Delivery*, vol. 32, no. 2, pp. 666–677, Apr. 2016.

[11] H. Liu, K. Ma, Z. Qin, P. C. Loh, and F. Blaabjerg, "Lifetime estimation of MMC for offshore wind power HVDC application," *IEEE J. Emerg. Sel. Topics Power Electron.*, vol. 4, no. 2, pp. 504–511, Jun. 2016.

[12] IEC61400-12-1, "Wind energy generation systems - Part12-1: Power performance measurements of electricity producing wind turbines."

[13] P. Milan, M. Wächter, and J. Peinke, "Stochastic modeling and performance monitoring of wind farm power production," *J. Renewable and Sustainable Energy*, vol. 6, no. 3, p. 033119, 2014.

[14] "ABB 5SNA 1200G450350," 2016. [Online]. Available: https://library.e.abb.com/public/afe3c7e548fe45ff8e4506203449f363/5SNA 1200G450350_5SYA 1415-04 03-2016.pdf

[15] N. C. Sintamarean, F. Blaabjerg, H. Wang, F. Iannuzzo, and P. De Place Rimmen, "Reliability oriented design tool for the new generation of grid connected PV-inverters," *IEEE Trans. Power Electron.*, vol. 30, no. 5, pp. 2635–2644, May. 2015.

[16] W. Conshohocken, "Standard Practices for Cycle Counting in Fatigue Analysis 1," vol. 85, no. Reapproved 2011, pp. 1–10, 2016.

[17] K. Mainka, M. Thoben, and O. Schilling, "Lifetime calculation for power modules, application and theory of models and counting methods," *in Proc. Power Electron. and Appl. (EPE)*, pp. 1–8, 2011.

[18] S. S. Manson and T. Dolan, "Thermal stress and low cycle fatigue," *J. Applied Mechanics*, vol. 33, p. 957, 1966.

[19] R. Bayerer, T. Herrmann, T. Licht, J. Lutz, and M. Feller, "Model for power cycling lifetime of igbt modules - various factors influencing lifetime," *in Proc. 5th Int. Conf. Integrated Power Electron. Systems*, Mar. 2008, pp. 1–6.

[20] I. F. Kovacevic, U. Drofenik, and J. W. Kolar, "New physical model for lifetime estimation of power modules," *in Proc. Int. Power Electron. Conf.- ECCE ASIA*, pp. 2106–2114, 2010.

[21] E. Özkol, S. Hartmann, and H. Duran, "Load-cycling capability of HiPak^{TM} IGBT modules 5SYA2043-03," Tech. Rep., 2012.

[22] M. A. Miner, "Cumulative damage in fatigue," *American Society of Mechanical Engineers - J. Applied Mechanics*, vol. 12, pp. 159–164, 1945.

[23] P. D. Reigosa, H. Wang, Y. Yang, and F. Blaabjerg, "Prediction of Bond Wire Fatigue of IGBTs in a PV Inverter under a Long-Term Operation," *IEEE Trans. Power Electron.*, vol. 31, no. 10, pp. 7171–7182, Oct. 2016.

[24] "Vestas V90 3.0 MW data.pdf." [Online]. Available: https://www.vestas.com/

[25] K. Ma, M. Liserre, F. Blaabjerg, and T. Kerekes, "Thermal loading and lifetime estimation for power device considering mission profiles in wind power converter," *IEEE Trans. Power Electron.*, vol. 30, no. 2, pp. 590–602, Feb. 2015.